ISSN 1392–1207. MECHANIKA. 2022 Volume 28(6): 481–489

Electro-Hydraulic Load-Sensitive Simulation Study of Walking Hydraulic System of Electric Agricultural Machinery

Hongyun MU*, Yanlei LUO, Yu LUO*****
**School of Mechanical Engineering, Guizhou University, Guiyang, Guizhou, 550025, China,*
E-mail: MUHONGYUNGZDX@163.com
***School of Mechanical Engineering, Guizhou University, Guiyang, Guizhou, 550025, China,*
E-mail: ylluo@gzu.edu.cn (Corresponding author)
****School of Mechanical Engineering, Guizhou University, Guiyang, Guizhou, 550025, China,*
E-mail: yluo6@gzu.edu.cn

crossref http://dx.doi.org/10.5755/j02.mech.31470

1. Introduction

With the increasing fuel cost in recent years, electricity as a renewable energy source has a lower price. Therefore, purely electric-driven agricultural machinery is a new product under the trend of protection of the environment. It uses electric motors instead of diesel engines, which can achieve actual zero emissions and meet increasingly stringent emission regulations. It combines agricultural and advanced information technology and uses computer systems to communicate with sensors. So that electric agricultural machinery can accurately complete various actions and realize the intellectualization of agricultural production [1].

The load-sensitive technology is one of the most widely used energy-saving hydraulic control systems. It uses the pressure feedback principle to feedback the maximum load pressure to the load-sensitive pump to adjust the flow rate balance of the system, thereby reducing the heating and energy loss of the system [2-4]. However, this conventional mechanical-hydraulic feedback control has low stability and drastic oscillations. Due to the use of long pipelines for feedback pressure, the system has a slow response and low efficiency, which deteriorate the system's performance [5, 6]. Many scholars have proposed electronically controlled load-sensitive systems based on sensors. They use high-speed switch valves instead of load-sensitive valves in load-sensitive pumps and electric signals instead of pressure signals, significantly improving the system's response speed, cost, control accuracy, and stability [7-11]. Zhongbao Cao proposed a load-sensitive hydraulic system anti-flow saturation control method to solve the flow saturation phenomenon when multiple actuators are combined. It detects the pressure at the pump source and the maximum load pressure through the pressure sensors and transmits these two pressure signals to the controller. The controller calculates the differential pressure between the two pressures. It indicates that the system meets the flow saturation condition when the pressure difference is less than the set pressure difference of the load-sensitive valve. The system will adopt complementary control strategies to adjust the gain of the pilot control handle input signal, reduce the main valve's open area, and achieve anti-flow saturation [12]. Hansen introduced the closed-loop feedback of the electrical pressure signal of the system based on the flow rate matching system and applied it to the forklift. The research results show that the system realizes the electro-hydraulic flow matching between the pump and valve and solves the flow matching error and other problems through the feedback of the electric pressure signal [13, 14]. Therefore, the pressure feedback type electro-hydraulic load-sensitive system adopts pressure sensors to detect and transmit pressure signals, which can solve the shortcomings caused by the long pipelines of conventional load-sensitive systems and improve the control accuracy of the system. Using a quantitative pump as a flow source can significantly reduce the agricultural machinery system's cost. However, the excess flow rate of the system will overflow back into the tank through the relief valve. It will increase the overflow loss of the system and reduce its efficiency of the system.

Tianliang Lin proposed a variable pressure difference control strategy based on a variable speed control quantitative pump load-sensitive system to reduce the energy consumption of pure electric-driven construction machinery and improve its work efficiency. They established a system simulation model and tested it on an 8 t electric drive excavator. Experimental results show that the proposed variable pressure difference control strategy based on variable speed control load-sensitive systems can reduce energy consumption and improve system controllability [15, 16]. Weiwei Wang compared the efficiency of the conventional quantitative pump of the throttling speed regulation, constant flow load-sensitive, and variable pump load-sensitive system through simulation experiments. The results show that the efficiency of the constant flow load-sensitive system is about 5% higher than the conventional quantitative pump of the throttling speed control system and is 22% lower than the variable pump load-sensitive system [17]. However, the quantitative pump's agricultural hydraulic system makes its cost lower than the load-sensitive pump. The combination of the permanent magnet synchronization motor (PMSM) and quantitative pump can solve the problem of high overflow loss of the pump. Compared with the mechanical structure control of a variable pump, it has the advantages of simple control, easy maintenance, and low cost.

Based on the above analysis, an electro-hydraulic load-sensitive (ELS) hydraulic drive chassis system for agricultural machinery is proposed. It uses a combination of PMSM and quantitative pump to replace the conventional combination of engine and load-sensitive pump. It uses a solenoid pressure compensation valve to replace the conventional pressure compensation valve. The system can realize variable LS differential pressure control and variable differential pressure control of the pressure compensation

valve through the pressure sensor's real-time feedback system pressure signal. It can effectively improve the performance of agricultural machinery to adapt to working conditions.

This paper is organized as follows. Section 2 introduces the system working principle. Section 3 introduces the component mathematical model analysis. Section 4 introduces the system modelling and simulation. Section 5 is the conclusions.

2. System working principle

2.1. Working principle of the ELS system

The ELS hydraulic drive chassis is proposed for agricultural machinery, as shown in Fig. 1. The system uses pressure sensors to detect system pressure in real time. They transmit the signal to controller 28 for processing, outputting the control signal of PMSM and solenoid pressure compensation valve, thus dynamically adjusting system pressure and flow rate to meet the demand of different working conditions. The system can realize variable LS differential pressure control and variable differential pressure control of the pressure compensation valve by setting Δp_{Ls} and Δp_d.

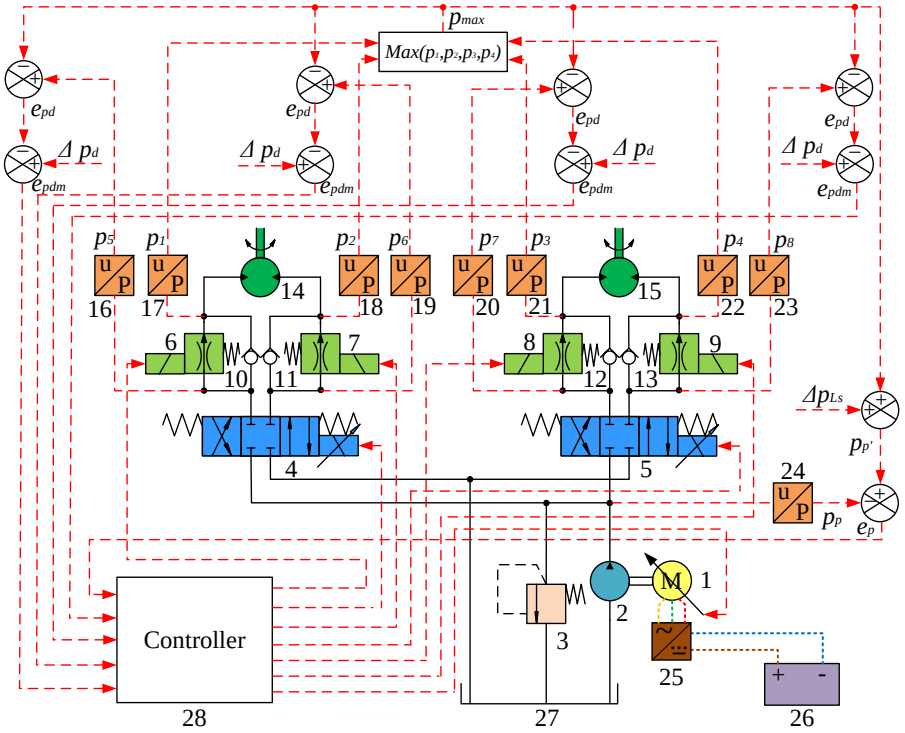

Fig. 1 ELS agricultural machinery hydraulic drive chassis schematic: *1* – PMSM; *2* - quantitative pump; *3* - relief valve; *4*, *5* - multi-way valve; *6*, *7*, *8*, *9* - solenoid pressure compensation valve; *10*, *11*, *12*, *13* - check valve; *14*, *15* - hydraulic motor; *16*, *17*, *18*, *19*, *20*, *21*, *22*, *23*, *24* - pressure sensor; *25* – inverter; *26* – supercapacitor; *27* – tank; *28* - controller

2.2. Principle of variable speed control

The system uses the PMSM and the quantitative pump, with pressure feed-back closed-loop control, thus achieving variable speed control, as shown in Fig. 2. The pressure sensors detect the maximum load pressure in real time. The quantitative pump output target pressure can be described as:

$$p_p^{'} = p_{Max} + \Delta p_{Ls}, \tag{1}$$

where: $p_p^{'}$ is the quantitative pump target pressure, Pa; p_{Max} is the maximum load pressure, Pa; Δp_{Ls} is the LS preset differential pressure, Pa.

The quantitative pump output pressure error can be described as:

$$e_p = p_p^{'} - p_p, \tag{2}$$

where: e_p is the quantitative pump output pressure error, Pa; p_p is the actual quantitative pump output pressure, Pa.

The PMSM target torque is obtained by inputting e_p to the PID1 controller for feedback control. The PMSM target torque can be described as:

$$T(e_p) = k_p e_p + k_i \int e_p dt + k_d \frac{de_p}{dt}, \tag{3}$$

where: $T(e_p)$ is the PMSM target torque, N.m; k_p is proportional value; k_i is integral value; k_d is differential value.

The PMSM target speed can be described as:

$$n_{ref} = f(e_p) = \frac{9550P}{T(e_p)}, \tag{4}$$

where: n_{ref} is the PMSM target speed, rev/min; P is the PMSM rated power, W.

When the PMSM target speed is dynamically changing, the PMSM actual speed also changes with it, thus dynamically controlling the quantitative pump outlet flow and pressure.

2.3. Principle of variable differential pressure control

Based on the above in Section 2.2 analysis, the system can follow the new Δp_{Ls} through pressure feedback closed-loop control when changing to new Δp_{Ls}. The flow rate through the multi-way valve can be described as follows, taking the system load maximum branch as an example:

$$Q = C_d \omega x \sqrt{\frac{2(\Delta p_{Ls} - \Delta p_d)}{\rho}}, \tag{5}$$

where: Q is the flow rate through the multi-way valve, m^3/s; C_d is the flow coefficient; ω is the spool area gradient; x is the multi-way valve spool displacement, m; Δp_d is the preset differential pressure of the pressure compensation valve, Pa; ρ is the oil density, kg/m^3.

From Eq. (5), it can be seen that when the system decreases Δp_{Ls}, it can reduce the system flow rate, thus reducing the system pressure loss and meeting the demand of low-speed and small-flow conditions. When the system increases Δp_{Ls}, it can effectively increase the system flow rate to meet the demand of high-speed and high-flow conditions.

2.4. Principle of variable differential pressure control of pressure compensation valve

The solenoid pressure compensation valve to replace the conventional pressure compensation valve can effectively improve the system response speed and control performance. The variable differential pressure control of the pressure compensation valve can be achieved by changing the preset differential pressure of the solenoid pressure compensation valve. The actual differential pressure of the solenoid pressure compensation valve can be described as:

$$e_{pd} = p_n - p_{Max}, \tag{6}$$

where: e_{pd} is the actual differential pressure of solenoid pressure compensation valve, Pa; p_n is the pressure before the solenoid pressure compensation valve, Pa.

The differential pressure error of the solenoid pressure compensation valve can be described as:

$$e_{pdm} = \Delta p_d - e_{pd}, \tag{7}$$

where: e_{pdm} is the differential pressure error of solenoid pressure compensation valve, Pa.

The control signal of the solenoid pressure compensation valve can be described as:

$$i = k_p e_{pdm} + k_i \int e_{pdm} dt + k_d \frac{de_{pdm}}{dt}, \tag{8}$$

where: i is the control signal of the solenoid proportional pressure compensation valve, mA.

When the control signal of the solenoid pressure compensation valve dynamically changes, the solenoid pressure compensation spool moves with it, thus controlling the solenoid pressure compensation valve to follow the new Δp_d.

Based on the above in Sections 2.2, Sections 2.3 and Sections 2.4 analysis, the variable LS differential pressure control and the variable differential pressure control of the pressure compensation valve can be realized by the closed-loop control of Δp_{Ls} and Δp_{Ls}. The system can better meet the requirements of different working conditions for electric agricultural machinery.

3. Component mathematical model analysis

3.1. PMSM mathematical model analysis

The PMSM is a typical nonlinear system with many internal variables and strong coupling. The equivalent schematic is shown in Fig. 3a. The stator voltage equation of the PMSM in three-phase stationary coordinates can be described as:

$$\begin{bmatrix} u_a \\ u_b \\ u_c \end{bmatrix} = \begin{bmatrix} R_s & 0 & 0 \\ 0 & R_s & 0 \\ 0 & 0 & R_s \end{bmatrix} \begin{bmatrix} i_a \\ i_b \\ i_c \end{bmatrix} + \begin{bmatrix} \psi_a \\ \psi_b \\ \psi_c \end{bmatrix}, \tag{9}$$

where: u_a, u_b and u_c are the three-phase stator winding voltage, V; i_a, i_b and i_c are the three-phase stator winding currents, A; ψ_a, ψ_b and ψ_c are the sum of the magnetic chains generated in the three-phase stator winding, Wb; R_s is the stator winding resistance, Ω.

The magnetic chain equation of the PMSM in the three-phase stationary coordinates can be described as:

$$\begin{bmatrix} \psi_a \\ \psi_b \\ \psi_c \end{bmatrix} = \begin{bmatrix} L_{aa} & M_{ab} & M_{ac} \\ M_{ba} & L_{bb} & M_{bc} \\ M_{ca} & M_{cb} & L_{cc} \end{bmatrix} \begin{bmatrix} i_a \\ i_b \\ i_c \end{bmatrix} + \psi_f \begin{bmatrix} \cos\theta \\ \cos\left(\theta - \frac{2\pi}{3}\right) \\ \cos\left(\theta + \frac{2\pi}{3}\right) \end{bmatrix}, \tag{10}$$

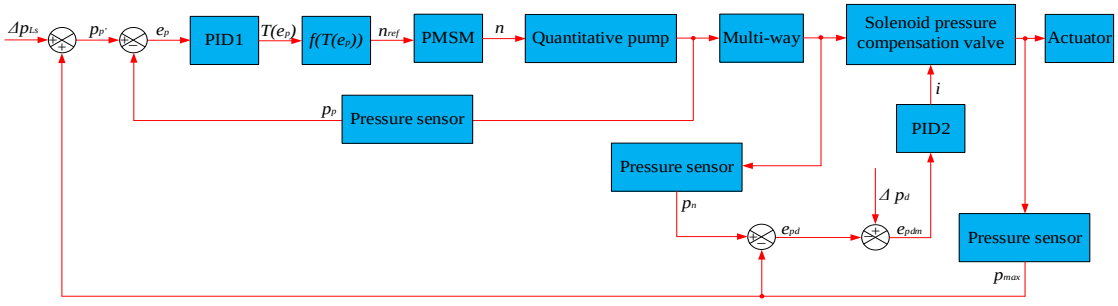

Fig. 2 Closed-loop control block diagram

where: M_{ab}, M_{ac}, M_{ba}, M_{bc}, M_{ca} and M_{cb} are the mutual inductance between windings, H; L_{aa}, L_{bb} and L_{cc} are the self-inductance of each winding, H; ψ_f is the rotor permanent magnetic linkage, Wb; θ is the rotor pole position, rad.

The electromagnetic torque vector equation of the PMSM in the three-phase stationary coordinates can be described as:

$$T_e = p_n \psi_f \, i, \tag{11}$$

where: T_e is the motor output torque, N.m; p_n is the number of motor poles.

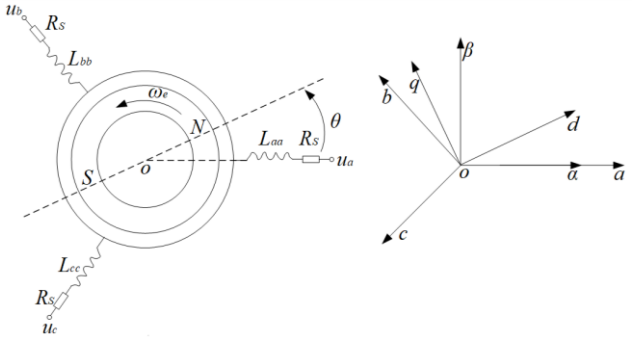

a b

Fig. 3 a - PMSM equivalent schematic; b - PMSM d-q coordinate transformation schematic

The α-β cartesian stationary coordinate system is introduced for facilitating vector analysis of PMSM, as shown in Fig. 3, b. It rotates synchronously with the rotor, and the d-axis coincides with the rotor magnetic pole. In the rotor *d-q* coordinate system, the stator current vector is decomposed into i_d and i_q. The two axes are orthogonal and independent of each other. The voltage equation can be described as:

$$\begin{bmatrix} u_d \\ u_q \end{bmatrix} = \begin{bmatrix} R_s & -\omega_e L_d \\ \omega_e L_d & R_s \end{bmatrix} \begin{bmatrix} i_d \\ i_q \end{bmatrix} + \frac{d}{dt} \begin{bmatrix} \psi_d \\ \psi_q \end{bmatrix} + \begin{bmatrix} 0 \\ \omega_e \psi_f \end{bmatrix}, \tag{12}$$

where: u_d, u_q are the d-p axis voltage, V; i_d, i_q are the d-p axis current, A; ψ_d, ψ_q is the d-p axis magnetic chains, Wb; ω_e is the rotor angular speed, rad/s.

The magnetic chains equation can be described as:

$$\begin{bmatrix} \psi_d \\ \psi_q \end{bmatrix} = \begin{bmatrix} L_d & 0 \\ 0 & L_d \end{bmatrix} \begin{bmatrix} i_d \\ i_q \end{bmatrix} + \begin{bmatrix} \psi_f \\ 0 \end{bmatrix}. \tag{13}$$

The electromagnetic torque equation can be described as:

$$T_e = \frac{3}{2} p_n \left[\psi_f \, i_q + \left(L_d - L_q \right) i_d i_q \right]. \tag{14}$$

The electromagnetic torque equation above is composed of two terms. Item first $\psi_f \, i_q$ is the excitation torque, the electromagnetic torque formed by the interaction between the permanent magnet excitation magnetic field and the stator current. The second term $\left(L_d - L_q \right) i_d i_q$ is the reluctance torque, the electromagnetic torque formed by the rotor saliency effect. The reluctance torque is inherent in the salient pole PMSM. For the non-salient pole PMSM $L_d \neq L_q$, it will not form reluctance torque. Therefore, the linear equation of electromagnetic torque can be described as:

$$T_e = \frac{3}{2} p_n \psi_f \, i_q. \tag{15}$$

The equation of motion can be described as:

$$T_e = T_L + J \frac{d\omega}{dt} + B\omega, \tag{16}$$

where: T_L is the load torque, N.m; J is the equivalent moment of inertia converted to the motor shaft, kg. m^2; ω is the mechanical angular speed of the motor output shaft, rad/s; B is the viscous friction coefficient.

The PMSM control principle can be obtained based on the above analysis, as shown in Fig. 4. The space vector pulse width modulation (SVPWM) vector control technology is used to control the PMSM. The control process is as follows: Detect and feedback the n and θ of PMSM. The target value of the q-axis current is obtained through PI speed control after comparing it with the target speed. The i_d and i_q are obtained after Clarke and Park transform the three current signals of the feedback stator. The u_d and u_q are obtained through PI current adjustment after comparing with the target current value of the d and q axes. The drive signal of the three-phase bridge circuit is obtained from the d and q axes voltage through SVPWM. The power switch of the drive bridge supplies power to the PMSM, thus generating electromagnetic torque to drive the PMSM.

3.2. Solenoid pressure compensation valve mathematical model analysis

One side of the solenoid pressure compensation valve is affected by the solenoid force, and the other is affected by the spring force. The opening of the solenoid pressure compensation valve is dynamically adjusted by controlling the size of the electromagnetic force to realize the pressure compensation function. The force balance equation of the solenoid pressure compensation valve can be described as:

$$F_e - F_s = M_c \ddot{x}_c + B_c \frac{dx_c}{dt} + K_{sc} x_c, \tag{17}$$

where: F_e is the solenoid force, N; F_s is the preset spring force of the solenoid proportional pressure compensation valve, N; M_c is the spool mass, kg; B_c is the spool viscous damping coefficient; K_{sc} is the spring stiffness of the right side of the pressure compensation; x_c is the spool displacement, m.

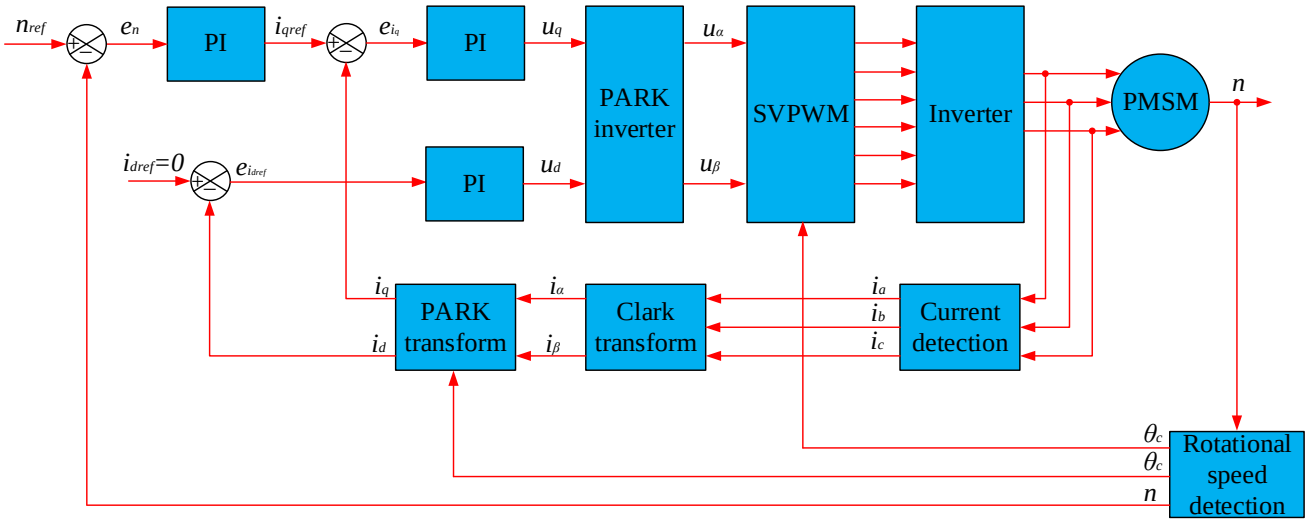

Fig. 4 PMSM control diagram schematic

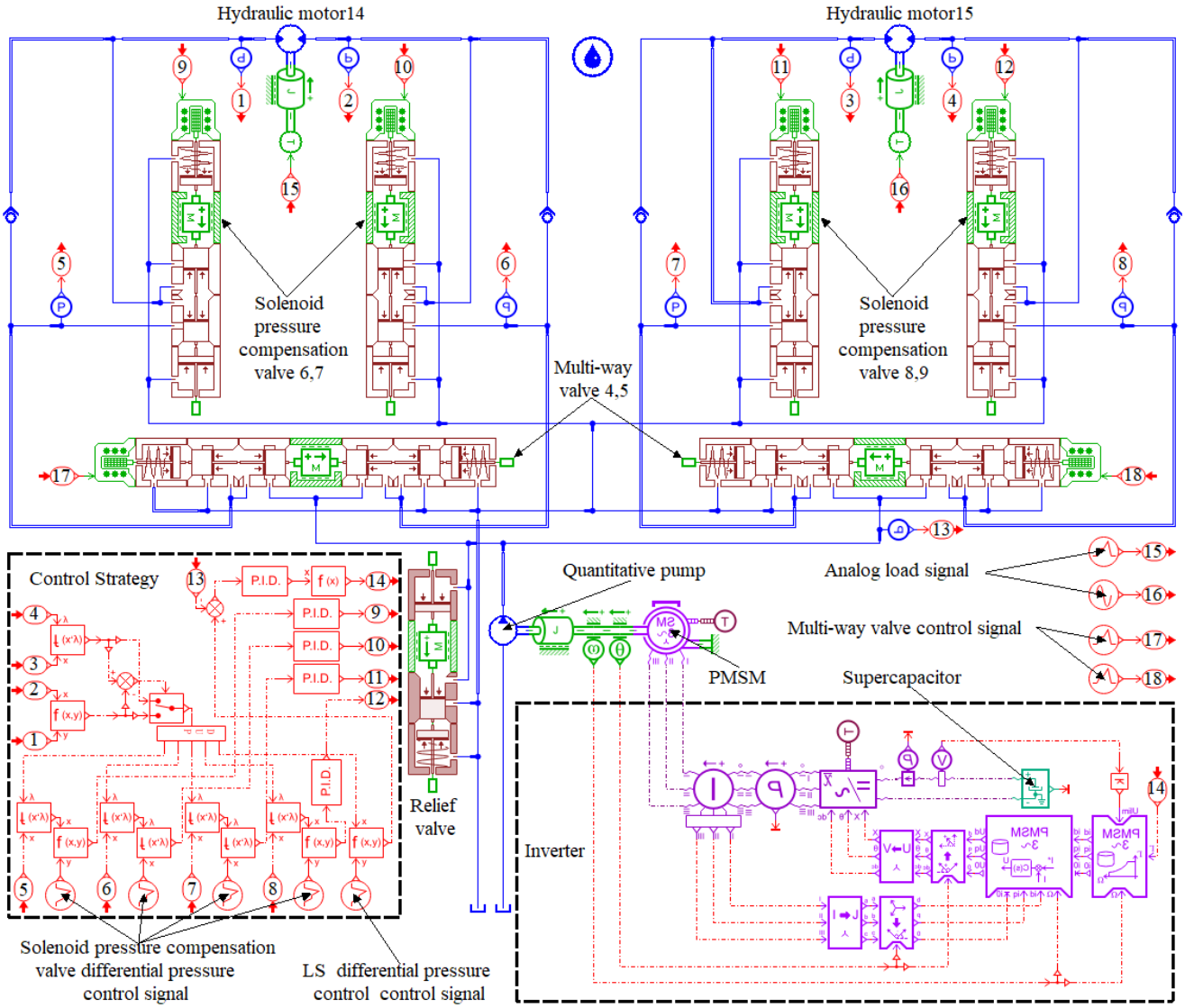

Fig. 5 AMESim simulation model

The F_e is controlled through e_{pdm}. According to Eqs. (7), (8) and (17), the solenoid pressure compensation valve realizes the function of pressure compensation when $e_{pdm} < 0$. The solenoid pressure compensation valve is closed when $e_{pdm} \geq 0$. According to the flow continuity principle, the flow rate through the multi-way valve equals the flow rate through the solenoid pressure compensation valve. The flow rate through the solenoid pressure compensation valve can be described as:

$$Q_m = Q = C_d \omega x \sqrt{\frac{2(\Delta p_{Ls} - \Delta p_d)}{\rho}}, \quad (18)$$

where: Q_m is the flow rate through the solenoid pressure compensation valve, m^3/s.

According to Eq. (18), when the Δp_d increases, the Q_m through the solenoid pressure compensation valve will decrease. Therefore, the flow rate of different system branches can be adjusted independently by changing the Δp_d.

4. System modelling and simulation

4.1. System modelling

Based on the schematic diagram of the hydraulic drive chassis of the ELS agricultural machinery in Fig. 1 and the schematic diagram of the closed-loop control in Fig. 2, the simulation model shown in Fig. 5 can be established by using AMESim. This research takes small and medium-sized self-propelled agricultural machinery as the simulation object. According to the walking velocity requirements of small and medium-sized self-propelled agricultural machinery, the simulation parameters of the hydraulic components of the system are determined. The system's variable differential pressure control range is determined according to the differential pressure range of the conventional load-sensitive system. Due to the complex working environment of agricultural machinery, the load of each branch of the system varies greatly. According to the traction and load of agricultural machinery, the load range distributed to each driving wheel is 10 N.m to 50 N.m. To better reflect the functional performance of the system, the load of the hydraulic motor 14 is set to 20 N.m, and the hydraulic motor 15 is set to $\left(20sin\left(\pi t\right)+30\right)$ N.m. Based on the above analysis, the system simulation parameters can be obtained, as shown in Table 1.

Table 1

Main parameters of the simulation model

Components	Parameters
Rated speed of PMSM	1500 rev/min
Displacement of quantitative pump	100 mL/rev
Displacement of hydraulic motor	50 mL/rev
LS preset differential pressure range	2.5~3.5 MPa
Preset differential pressure range of solenoid pressure compensation valve	1~2 MPa

4.2. Analysis of compound action

The Δp_{Ls} is set to 3 MPa, and Δp_d is set to 1.5 MPa. The multi-way valve 4 is fully open from 0 to 1 s, half open from 1 s to 4 s, and fully open from 4 s to 5 s. The multi-way valve 5 is half open from 0 to 2 s, fully open from 2 s to 3 s, and half open from 3 s to 5 s. The simulation time is set to 5 s.

The outlet pressure of the quantitative pump can change with the change of the maximum load pressure, and the LS pressure difference is kept at 3 MPa, as shown in Fig. 6. The differential pressure between the multi-way valves 4 and 5 are kept at 1.5 MPa because of the compensation function of the solenoid pressure compensation valve. The flow rate of the corresponding hydraulic motor increases when the opening of the multi-way valve increase, as shown in Fig. 7. The flow rate of the corresponding hydraulic motor decreases when the opening of the multi-way valve decreases. The flow rate of the relief valve is 0. To sum up, the flow rate of each branch is independent of the load and proportional to the opening of the multi-way valve. There are no overflow losses in this system. The system realizes the essential functions of the conventional load-sensitive system.

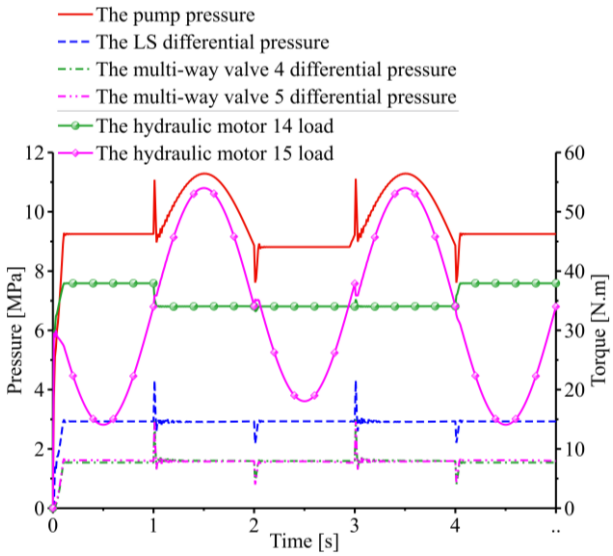

Fig. 6 System differential pressure and load curves

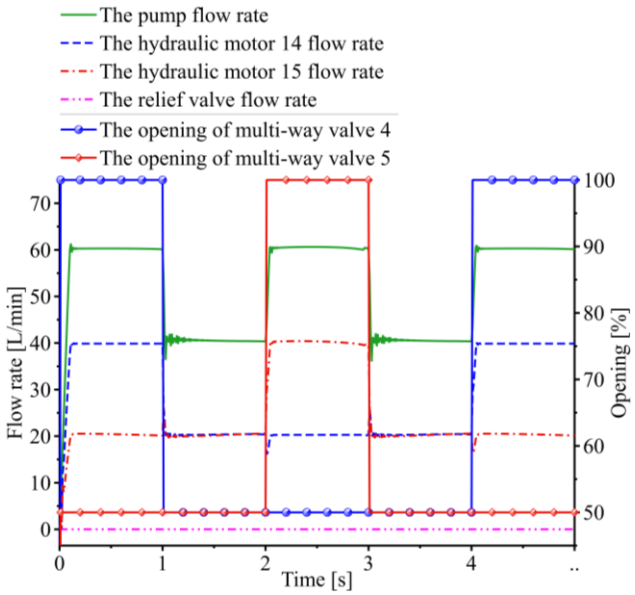

Fig. 7 Hydraulic motor flow and multi-way valve opening curves

4.3. Analysis of variable LS differential pressure control

The Δp_d is set to 1.5 MPa. The Δp_{Ls} is set to 3 MPa from 0 to 1s, 2.5 MPa from 1 s to3 s, and 3.5 MPa from 3 s to 5 s. The multi-way valves 4 and 5 are fully open. The flow rate of hydraulic motors 14 and 15 increases when the Δp_{Ls} increase, as shown in Fig. 8. The flow rate of hydraulic motors 14 and 15 decreases when the Δp_{Ls} decrease. The flow rate of hydraulic motors 14 and 15 are the same during the change. It is consistent with the analysis in

Section 2.3, which verifies the feasibility of variable LS differential pressure control. The system response speed increases when the Δp_{Ls} increase, as shown in Fig. 9. The PMSM output power decreases when the Δp_{Ls} decrease. To sum up, for straight driving conditions of agricultural machinery. The Δp_{Ls} is increased to increase the system flow rate and response speed when the system is in high-speed and high-flow conditions. The system is capable of a wide range of no-flow saturation functions. The Δp_{Ls} is decreased to reduce system pressure loss and energy consumption when the system is in low-speed and small-flow conditions.

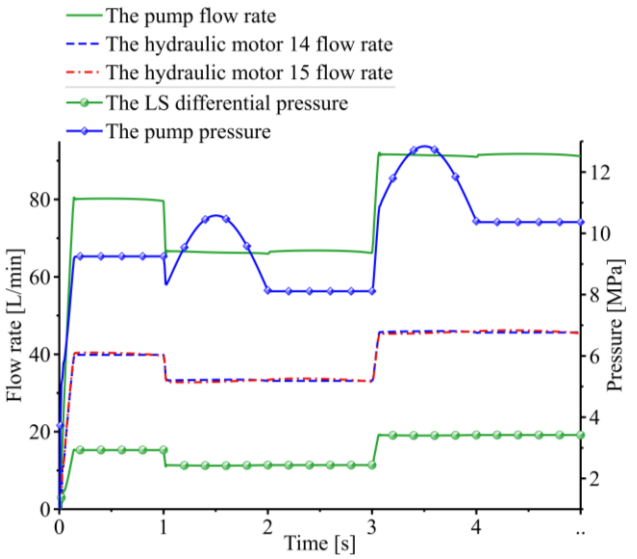

Fig. 8 Hydraulic motor flow rate and system differential pressure curves

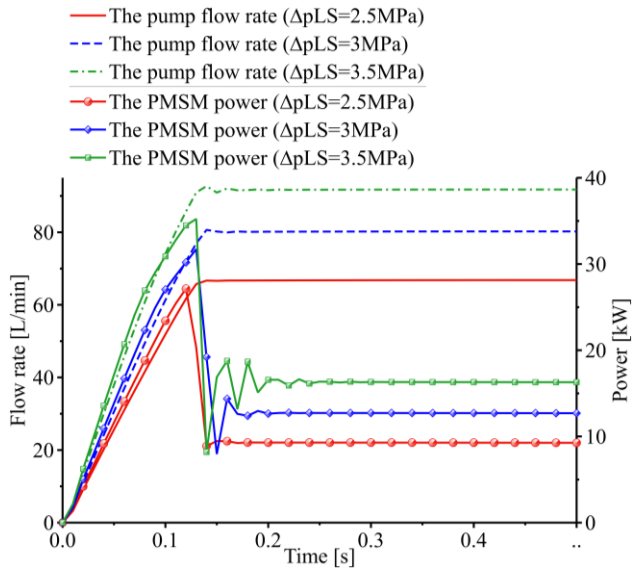

Fig. 9 Different Δp_{Ls} pump flow rate and PMSM power curves

4.4. Analysis of variable differential pressure control of pressure compensation valve

Change Δp_{Ls} can effectively improve agricultural machinery's driving speed adjustment range under straight driving conditions. Still, when agricultural machinery is under steering conditions, it cannot meet the requirements. Therefore, a variable Δp_d control is proposed based on variable Δp_{Ls} control. The Δp_{Ls} is set to 3 MPa. The Δp_d is set to 1.5 MPa from 0 to 1 s, 1 MPa from 1 s to 3 s, and 2 MPa from 3 s to 5 s on the left branch. The Δp_d is set to 1.5 MPa from 0 to 2 s, 2 MPa from 2 s to 4 s, and 1 MPa from 4 s to 5 s on the right branch. The multi-way valves 4 and 5 is fully open.

Figs. 10 and 11 show that when the Δp_d increases, the differential pressure of the corresponding multi-way valve decreases, and the branch flow rate decreases. When the Δp_d decreases, the differential pressure of the corresponding multi-way valve increases, and the branch flow rate increases. It is consistent with the analysis in Section 2.4, which verifies the feasibility of variable Δp_d control. As shown in Fig. 12 show that when Δp_d increases, the output power of PMSM decreases. To sum up, for steering conditions of agricultural machinery, variable Δp_d control can adjust a branch's flow rate independently to improve the steering performance of agricultural machinery. The system energy consumption can be effectively decreased when decreasing Δp_d.

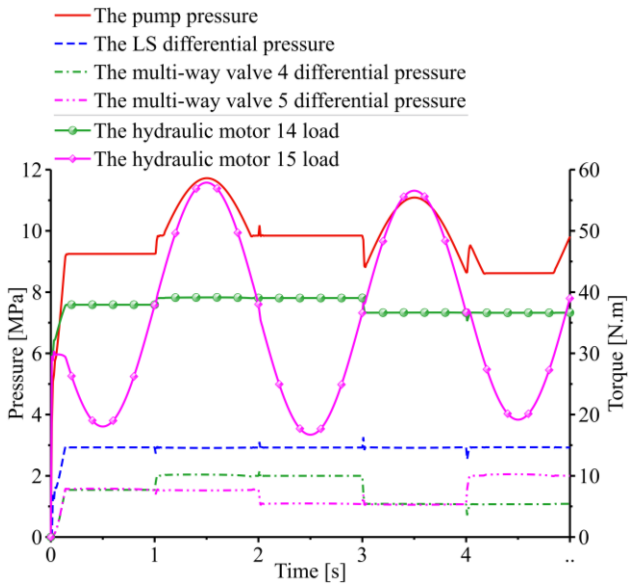

Fig. 10 System differential pressure and load curves

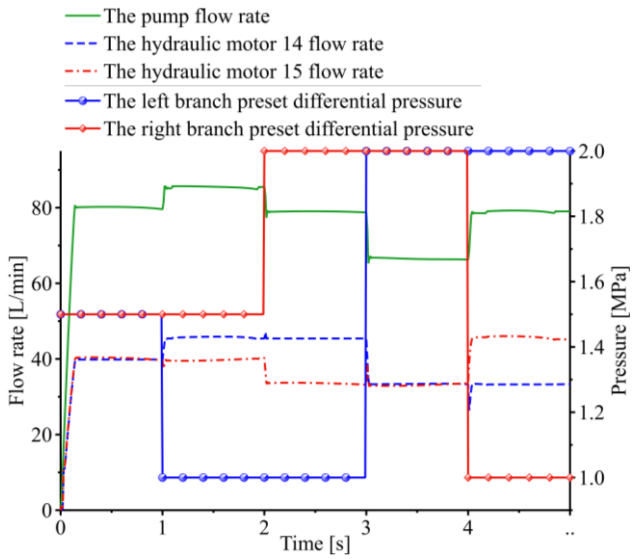

Fig. 11 Hydraulic motor flow rate and system preset differential pressure curves

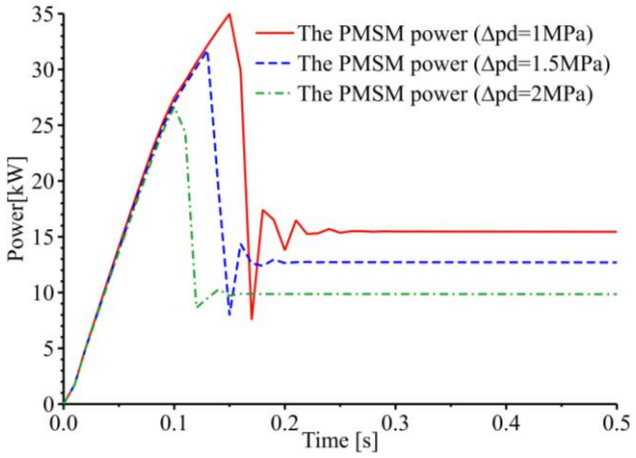

Fig. 12 Different Δp_d PMSM power curves

5. Conclusions

The principle of hydraulic drive chassis and variable differential pressure control of agricultural machinery are analyzed, and the system model is established. The following conclusions can be gained:

1. The flow rate of each branch is independent of the load and proportional to the opening of the multi-way valve. There are no overflow losses in this system. The system realizes the essential functions of the conventional load-sensitive system.

2. For straight driving conditions of agricultural machinery. The Δp_{Ls} is increased to increase the system flow rate and response speed when the system is in high-speed and high-flow conditions. The system is capable of a wide range of no-flow saturation functions. The Δp_{Ls} is decreased to reduce system pressure loss and energy consumption when the system is in low-speed and small-flow conditions.

3. For steering conditions of agricultural machinery, variable Δp_d control can adjust a branch's flow rate independently to improve the steering performance of agricultural machinery. The system energy consumption can be effectively decreased when decreasing Δp_d.

4. Variable Δp_{Ls} and Δp_d control is feasible and can effectively improve the adaptability of agricultural machinery under different working conditions. It can effectively reduce the system energy consumption and provide a theoretical basis for the intellectualization of electric agricultural machinery.

Acknowledgments

This work is supported by the Key Topics of Teaching Reform of Postgraduate Education in Guizhou Province (YJSCXJH (2020) 006), Science and Technology Project of Guizhou Province (Qiankehe Foundation-ZK [2022] General 087), National Natural Science Foundation of China Project (52265007), the State Scholarship Fund of China (201906675018), National Natural Science Foundation of China Project (51965011).

References

1. **He, Y.; Xing, Z.; Hou, H.; & Wu, X.** 2019. Development status and prospect of intelligent agricultural machinery equipment, Journal of Agricultural Science and Technology (Beijing) 21(6): 8-19. https://dx.doi.org/10.13304/j.nykjdb.2018.0481.
2. **Xie, H.; Liu, Z.; & Yang, H.** 2016. Pressure regulation for earth pressure balance control on shield tunneling machine by using adaptive robust control, Chinese Journal of Mechanical Engineering 29(3): 598-606. https://dx.doi.org/10.3901/CJME.2016.0330.042.
3. **Huang, W. N.; Quan, L.; & Huang, J. H.** 2016. Excavator swing system controlled with separate meter-in and meter-out method, Journal of Mechanical Engineering 52(20): 159-167. https://dx.doi.org/10.3901/JME.2016.20.159.
4. **Pedersen, H. C.; Andersen, T. O.; & Hansen, M. R.** 2004. Load sensing systems-a review of the research contributions throughout the last decades, Proceedings 4th IFK Workshop, pp. 125-139.
5. **Wu Du-qiang.** 2003.Modeling and experimental evaluation of a load-sensing and pressure compensated hydraulic system, Saskatoon: University of Saskatchewan. http://dx.doi.org/10388/etd-12032003-134850.
6. **Huang, H.** 2008. Research on The Energy-saving Control System of Hydraulic Excavator Based on Load-sensing Technologies. Jilin: Jilin University.
7. **Quanyi, H.; Hong, Z.; Shujun, T.; & Xuxin, Q.** 2017. Performances analysis of a novel load-sensing hydraulic system with overriding differential pressure control, Proceedings of the Institution of Mechanical Engineers, Part C, Journal of Mechanical Engineering Science 231(23): 4331-4343. https://dx.doi.org/10.1177/0954406216667760.
8. **Min, C. A.; Jz, B.; Bing, X. B.; & Rd, C.** 2020. An electrohydraulic load sensing system based on flow/pressure switched control for mobile machinery, ISA Transactions 96: 367-375. https://dx.doi.org/10.1016/j.isatra.2019.06.018.
9. **Shi, J.; Quan, L.; Zhang, X.; & Xiong, X.** 2018. Electro-hydraulic velocity and position control based on independent metering valve control in mobile construction equipment, Automation in Construction 94: 73-84. https://dx.doi.org/10.1016/j.autcon.2018.06.005.
10. **Ding, R.; Zhang, J.; Xu, B.; & Cheng, M.** 2018. Programmable hydraulic control technique in construction machinery: Status, challenges and countermeasures, Automation in Construction 95: 172-192. https://dx.doi.org/ 10.1016/j.autcon.2018.08.001
11. **Cheng, M.; Zhang, J.; Xu, B.; & Ding, R.** 2018. Electrohydraulic load sensing system via compound control of flow feedforward and pressure feedback, J. Mech. Eng. 54: 262-270. https://dx.doi.org/10.3901/JME.2018.20.262.
12. **Cao, Zhong-bao.** 2009. Research on the Flow-Saturated Resistant Control Technology of Load-Sensing Hydraulic System. Dalian: Dalian University of Technology.
13. **Hansen, M. R.; Andersen, T. O.; Pedersen, H. C.** 2006, January. Robust electric load sensing applied to an open circuit axial piston pump, ASME International Mechanical Engineering Congress and Exposition 47713: 1-8. https://dx.doi.org/10.1115/imece2006-13033.
14. **Hansen, R. H.; Iversen, A. M.; Jensen, M. S.; Andersen, T. O.; & Pedersen, H. C.** 2010. Modeling and control of a teletruck using electronic load sensing, Engineering Systems Design and Analysis 49170: 769-778). https://dx.doi.org/10.1115/esda2010-25270.

15. **Sheng-jie, F. U.; Tian-liang, L. I. N.; Lang, W. A. N. G.; & Cheng, M. I. A. O.** 2020. Load sensitive system based on variable speed control, China Journal of Highway and Transport 33(5): 189. https://dx.doi.org/10.19721/j.cnki.1001-7372.2020.05.017.
16. **Fu, S.; Wang, L.; & Lin, T.** 2020. Control of electric drive powertrain based on variable speed control in construction machinery, Automation in Construction 119: 103281. https://dx.doi.org/10.1016/j.autcon.2020.103281.
17. **WANG Wei-wei.** 2011. Load Sensitive System Dynamic Characteristics and Energy-saving Analysis. Qinhuangdao: Yanshan University.

H.Y. Mu, Y.L. Luo, Y. Luo

ELECTRO-HYDRAULIC LOAD-SENSITIVE SIMULATION STUDY OF WALKING HYDRAULIC SYSTEM OF ELECTRIC AGRICULTURAL MACHINERY

S u m m a r y

The conventional load-sensitive hydraulic drive chassis system for agricultural machinery uses a combination of engine and load-sensitive pump, which cannot adjust the control strategy according to the working conditions. It does not meet the current trend of energy-saving and emission reduction. To this end, an electro-hydraulic load-sensitive hydraulic drive chassis system for agricultural machinery, which uses a combination of permanent magnet synchronous motor and quantitative pump, is proposed. A variable LS differential pressure control and a variable differential pressure control of the pressure compensation valve to improve agricultural machinery's working performance are proposed. AMESim is used to establish the system simulation model to obtain the system composite motion, variable LS differential pressure control, and variable pressure differential control of the pressure compensation valve performance. The simulation results show that the system achieves the essential functions of a conventional load-sensitive system. The variable LS differential pressure control and the variable pressure differential control of the pressure compensation valve are feasible. They can effectively improve the performance of agricultural machinery to adapt to working conditions. It can effectively reduce the system energy consumption and provide a theoretical basis for the intellectualization of electric agricultural machinery.

Keywords: electric agricultural machinery, ELS walking system, PMSM; variable LS differential pressure control, variable differential pressure control of pressure compensation valve, AMESim.

Received May 24, 2022
Accepted November 28, 2022